Petrology, Vol. 4, No. 3, 1996, pp. 307–317. Translated from Petrologiya, Vol. 4, No. 3, 1996, pp. 326–336.

Incompatible Element Partitioning between Clinopyroxene and Basalt Liquid Revealed by the Study of Melt Inclusions in Minerals from Troodos Lavas, Cyprus

A. V. Sobolev, A. A. Migdisov, and M. V. Portnyagin

Vernadsky Institute of Geochemistry and Analytical Chemistry, Russian Academy of Sciences, ul. Kosygina 19, Moscow, 117975 Russia

Received November 20, 1995

Abstract—Melt inclusions in clinopyroxene from Troodos lavas were studied by the methods of high-temperature optical thermometry, secondary ion mass spectrometry, and microprobe analysis to determine the partition coefficients of Ba, Sr, Y, Ti, La, Ce, Nd, Sm, Dy, Er, and Yb between low-Al, high-Mg clinopyroxene and boninite-like melt for temperatures of 1100–1190°C and a hydrous fluid pressure of 1 kbar. Variations of the partition coefficients were found as a function of the temperature and the Al_2O_3 content in clinopyroxene. The results proved the study of melt inclusions in minerals to be an efficient tool for determining the coefficients of trace element distribution between the crystalline phase and the liquid.

INTRODUCTION

The last years have witnessed a growing interest of petrologists and geochemists in modeling magmatic processes. One of the reasons is that the observed products of igneous activity (rocks, quench glasses) were proven to have suffered intricate, unobservable transformations after the magmas were produced by the melting of the mantle (Johnson *et al*., 1990; Johnson and Dick, 1992). The reconstruction of primary melt compositions and the simulation of the processes of melting (Johnson *et al*., 1990; Johnson and Dick, 1992) or metasomatism (Navon and Stolper, 1987) of mantle source requires knowledge of the coefficients K_d of trace element partitioning between the crystalline phase and the melt. Of particular interest is the determination of K_d values for clinopyroxene: of all crystalline phases in equilibrium with mantle melts, clinopyroxene is known to be the most enriched in incompatible elements, and, hence, its setting excerts the greatest effect on the composition of the resulting melt.

There are numerous publications on the determination of the partition coefficient between clinopyroxene and the melt [see review papers of Green (1994) and Hack *et al*. (1994)]. Some of them are based on studies of natural rocks (usually the system phenocryst–groundmass), and others utilize experimental studies of model systems. The main problem of the former approach is whether the phenocrysts and groundmass were in equilibrium, which sometimes is far from evident because of the great variability of magmatic systems in terms of the contents of incompatible elements (Sobolev and Shimizu, 1993; Sobolev, 1996; Portnyagin *et al*., 1996). Moreover, such studies are hampered by difficulties in correctly evaluating the crystallization parameters. The experimental approach is aggravated, in addition to proving phenocryst–groundmass equilibrium, by the difficulty of determining trace element concentrations in clinopyroxene because of the small size (usually a few dozen microns) and zoning of its crystals. This problem is solved by the artificial addition of incompatible elements with concentrations that can be measured with an electron microprobe (e.g., Hack *et al*., 1994) or by means of natural alkalic melts enriched in incompatible elements (e.g., Hart and Dunn, 1993). In both instances, the results may be inapplicable to natural magmas poor in incompatible elements, because of the deviation of the systems from Henry's law, where the concentrations of elements are too high (Green, 1994), or because of the "capture effect" (Urusov *et al*., 1993), where their contents are too low.

Most of the above problems can be solved by the thermometrical study of melt inclusions in minerals in combination with the modern techniques of local microanalysis. This is possible, in the first place, because the method of melt inclusion homogenization is able to determine crystallization temperature and the compositions of the coexisting melt and crystalline phase (Roedder, 1984). Secondly, the equilibrium of the host mineral and the included melt can be proven by the major components or demonstrating the homogeneity of both phases in terms of trace elements. Thirdly,

K_d is determined for natural concentration levels. Nevertheless, this approach has its own problems: the parameters of melt crystallization and composition can be distorted (Sobolev and Danyushevsky, 1994), or the melt can be heterogeneous in composition at the contact with the growing crystal (Roedder, 1984). Therefore, the results for each object under study must be verified.

The goal of this study was to assess the possibility of combining the homogenization of melt inclusions with the modern methods of local microanalysis (ion and electron probes) for determining the distribution coefficients of incompatible elements between clinopyroxene and the melt. The results have shown that this combination yields numerical data, and offers promise as an efficient tool.

OBJECT OF STUDY

In this study, we used low-Al clinopyroxenes and water-bearing boninite-like melts from the Upper lavas of the Troodos Massif, Cyprus, typical of the early stages of island-arc evolution (Sobolev *et al.*, 1993). The basis for this choice was the lack of experimentally determined K_d for these compositions, on the one hand, and the necessity to have such data to be able to reconstruct the compositions of melts that were in equilibrium with the clinopyroxenes of the Troodos intrusive complex (Batanova *et al.*, 1996), on the other. Samples of melt inclusions and host clinopyroxenes were collected from the Mitsero village (sample TRV-191), the Pedieous River (samples TRD-133 and TRD-135), and the Scoriotissa Mine (sample TRV-200) areas. The rocks are porphyritic olivine and clinopyroxene picrites and picrobasalts. The olivine of all rocks is carbonized. The clinopyroxene accounts for 10 to 40% of the rock volume, and occurs as euhedral crystals (up to 5 cm across) or glomerophyric aggregates of equant crystals.

The clinopyroxene phenocrysts contain primary inclusions of melt, crystalline phases (chromian spinel and olivine), and low-density fluid. The melt inclusions usually occur as accumulations of dozens of individual inclusions of varying sizes (a few to 200 μm). They are smooth, negatively faceted ellipsoids; less common are elongated and amebiform varieties. They are partially crystallized in all samples. Ferroan clinopyroxene, glass, Al-spinel, amphibole, and low-density fluid were identified in them.

METHODS OF STUDY

Thermometry

The fundamentals of the method of melt inclusion homogenization have been described fairly comprehensively in literature (e.g., Roedder, 1984; Sobolev *et al.*, 1993). When applied to fluid-saturated systems, this technique yields realistic values of crystallization temperatures and crystallizing melt compositions. The accuracy criteria of the results obtained are the relations between the homogenization temperatures of melt inclusions and host mineral compositions and the attainment of equilibrium between them (Sobolev *et al.*, 1993; Sobolev and Danyushevsky, 1994).

In this study, we used an experimental procedure designed for hydrous melts (Sobolev and Danyushevsky, 1994). Its essence is to minimize the time of the experiment to prevent H_2O dissipation in melt inclusions as H_2 diffuses through the host mineral. The time of the experiment at $T > 1000$°C was not more than 5 min. The following phase transformations were observed: glass devitrification at 500–550°C, the beginning of melting at 550–600°C, and the melting of the last daughter crystal at 1100–1150°C. The complete homogenization of the inclusions occurred after the fluid phase dissolution, 30–50°C after the melting of the last crystal. The inclusions were quenched at the homogenization temperature.

Electron Microprobe Analysis

The quenched homogenized melt inclusions and the host clinopyroxenes were analyzed at the Vernadsky Institute of Geochemistry and Analytical Chemistry, Russian Academy of Sciences, using a Camebax Microbeam microprobe under conventional experimental conditions: 15 kV, 5–20 nA, and international glass (USNM 111240/52) and clinopyroxene (USNM 122142) standards (Jarosewich *et al.*, 1980). Each phase was analyzed at three points with 5×5 μm scanning.

Secondary Ion Mass Spectrometry

Trace elements were determined in the homogenized melt inclusions and host clinopyroxenes using a SIMS (All-Russian Institute of Mineral Reserves) technique and an IMS-4f probe at the Institute of Microelectronics, Russian Academy of Sciences, Yaroslavl'. The measurement procedure was described by Sobolev and Batanova (1995). The primary beam diameter was 20 μm. The clinopyroxene composition was determined at three points within a range of 30–200 μm around the inclusion. The melt inclusions were analyzed at one point in the center of the inclusion. Each data point was an average of five analyses over a vertical profile 10–15 μm deep with the integration time of approximately 40–60 min.

Figure 1a and Table 1 present data on the glass and clinopyroxene standard reproducibility which was determined by a replicate analysis performed for each series of 4–5 analyses. The measurement error was less than 10% for most of the elements with a more than 0.1 ppm content and 30–50% for lower concentrations (<0.1 ppm). The quality of the analytical data was verified additionally by comparing the Ti concentrations measured with the ion and the electron probe (Fig. 1b).

H_2O was determined using a SIMS technique described by Sobolev (1996) with a <10% error.

RESULTS

Crystallization Conditions

Clinopyroxene crystallization temperature was determined by the homogenization of primary melt inclusions. The occurrence of syngenetic fluid inclusions justified the assumption that the melt is fluid saturated and, hence, the equation of the melt homogenization temperature with the fluid capture temperature (Roedder, 1984). The resulting 1100–1190°C range of crystallization temperatures was consistent with the values obtained earlier for clinopyroxene from the upper Troodos lavas (Sobolev *et al*., 1993). The good correlation between the clinopyroxene crystallization temperature and composition (Fig. 2a) indicates that the temperature measurement error was not more than 10°C.

Clinopyroxene crystallization pressure was determined by a technique described by Nimis (1995) and found to be 1.2 ± 0.5 kbar. An independent estimate of 0.9 ± 0.4 kbar was obtained for the aqueous fluid pressure using the H_2O contents in the melt inclusions and Burnham's model (Burnham, 1975). The agreement of these values, within the precision of the techniques used, is additional proof of the accuracy of the results.

Compositions of Melt Inclusions and Host Minerals

Major elements. The comparison of the electron microprobe data obtained at different points of the measured phases suggests that they are chemically uniform within the accuracy of the analysis (Table 2). In terms of the major element contents, the homogenized melt inclusions correspond to the water-bearing boninite-like magma of the northern Troodos lavas (Sobolev *et al*., 1993). The clinopyroxenes are of a low-Al, high-Mg variety. As seen in Fig. 3, the homogenized melt inclusions are in equilibrium with the host clinopyroxenes.

Trace elements. As follows from the data listed in Table 3, most of the standard deviations from the mean trace element contents in the clinopyroxenes and glasses are not higher than 20% for the concentrations above 0.1 ppm. Only for the lowest Ba and La contents in clinopyroxene (0.01–0.05 ppm) were they found to be higher than 40%. These values are compatible with the standard reproducibility data (Table 1, Fig. 1), and prove that the objects under study are highly homogeneous.

The contents of incompatible elements in the melt inclusions (Table 3, Fig. 4) exhibit features typical of suprasubduction lavas, in particular, of the boninite-like lavas of the northern Troodos Massif (Sobolev *et al*., 1993): depleted REE patterns and positive anomalies in the LILE (Ba, Sr, and K) contents. The clinopyroxenes feature differentiated patterns with depletion of the most incompatible elements and a considerable negative Zr anomaly.

Table 1. Composition (ppm) and reproducibility of reference standards

Elements	KH-1	R, %	30-2	R, %
Ba	0.36	47.7	178	3.7
La	1.68	0.9	12.95	3.7
Ce	5.56	0.6	27.42	2.6
Sr	49	1.1	248	2.9
Nd	5.99	2.5	15.26	3.4
Zr	24	1.8	102	1.8
Sm	2.08	7.1	3.73	5.3
Ti	5200	0.4	8917	1.3
Dy	2.78	4.5	4.03	3.3
Er	1.50	20.1	2.46	13.5
Y	13	0.2	20.15	0.6
Yb	1.23	1.0	2.37	3.3

Note: KH-1—clinopyroxene (Kilbourn Hall, New Mexico, USA); 30-2—basalt glass from the mid-ocean ridge at 14°N. Rare earth elements were determined in the standards by isotope dilution at the Geological Institute of Kola Research Center, Russian Academy of Sciences, Apatity (analyst Yu.A. Balashov). Sr, Zr, Ti, and Y were determined in the KH-1 clinopyroxene by Micro-PIXE analysis (Czamanske *et al*., 1993). Ba was determined in clinopyroxene, and Ti, Zr, Y, Sr, and Ba were determined in glass by the SIMS method at Woods Hole Oceanographic Institution, Woods Hole, USA (analyst N. Shimizu). Here and in Table 3, R, % is the SIMS measurement error of standards obtained in this study.

Partition Coefficients of Incompatible Elements between Clinopyroxene and Melt

The crystallization and composition ranges of the phases were narrow enough to use, as a first approximation, the K_d values averaged for the entire series of experiments. These K_d values (Fig. 5, Table 3) fit within the range of values reported in the literature and show the usual behavior: the monotonic K_d decreases with the increasing incompatibility of the elements and the abnormally high K_d value for Zr. They also show a systematic tendency to be shifted into the region of lower values compared with the data reported for high-Al-clinopyroxenes at high pressures and temperatures (Hart and Dunn, 1993; Johnson, 1994).

Hack *et al.* (1994) reported an inverse relationship between ln (K_d) and the temperature defined by the known expression of the equilibrium constant as thermodynamic potentials (Wood and Fraser, 1977). In this paper, an attempt is made to describe this relationship numerically, as a second approximation of the K_d evaluation.

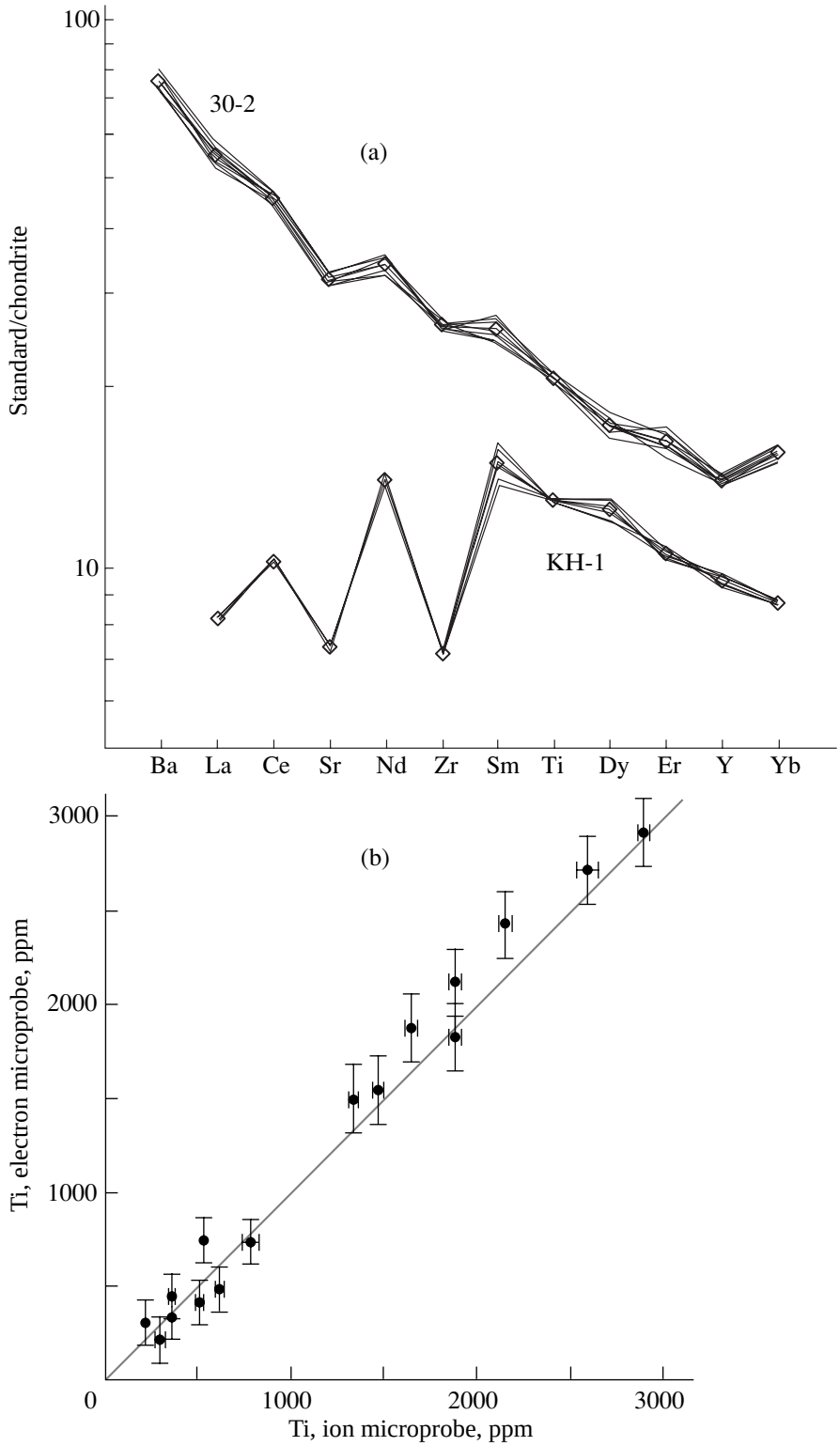

Fig. 1. Demonstration of the reproducibility and correctness of analytical data.

(a) Normalized trace element contents for the analyses of the 30-2 basalt glass and KH-1 clinopyroxene standards. The rhombs denote reference contents standardized by isotope dilution. The elements were determined by the SIMS method; their contents were normalized to chondrite (Anders and Grevess, 1989).

(b) Comparison of Ti concentrations (ppm) in clinopyroxenes and melt inclusions obtained by SIMS and electron microprobe analysis. The measured concentration errors displayed hereinafter are standard deviations.

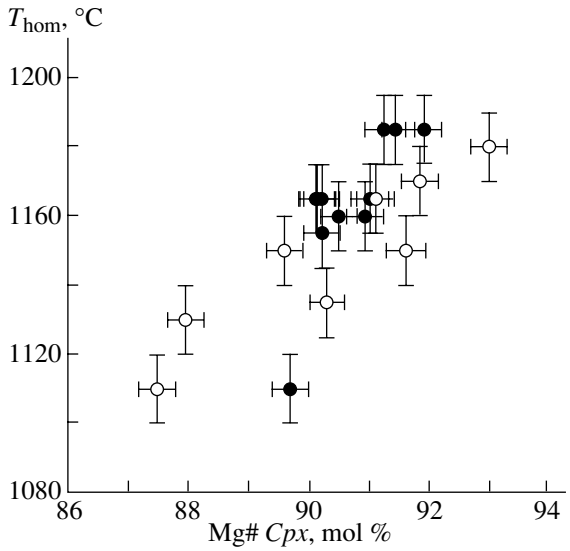

Fig. 2. Variation of the homogenization temperature of melt inclusions with the composition of the host clinopyroxene.
Open circles show inclusions analyzed by the SIMS method. Mg# = Mg/(Mg + Fe).

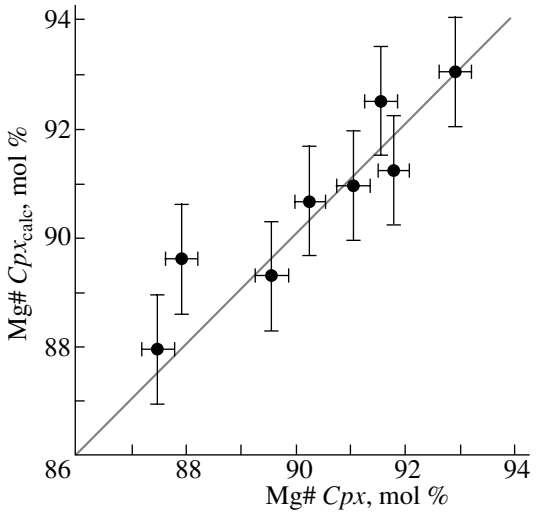

Fig. 3. Comparison between the compositions of the host clinopyroxene and the clinopyroxene coexisting with homogenized melt inclusions.
The calculation was performed using the model of Nielsen and Drake (1979) for $Fe^{2+}/Fe^{3+} = 7$ in the melt, the value derived from the data reported by Sobolev *et al.* (1993).

Figure 6 presents the $\ln K_d$ variation as a function of inverse crystallization temperature. We computed the parameters of the linear regression equation

$$\ln(K_d) = A \times 10000/(T, K) + B$$

for each element (Table 4).

The correlation coefficients for Zr and La are close to the significance limit. The correlation for Ba is insignificant. The other elements show strong correlation.

Table 2. Composition (wt %) of homogenized inclusions and host clinopyroxenes: major elements

Oxide	TRD-135/1*	TRD-135/3	TRV-191/9	TRV-191/13	TRD-133/15	TRV-200/16	TRV-200/19	TRV-200/20
Inclusions								
SiO_2	52.48	53.54	55.20	55.83	53.59	55.40	54.60	51.47
TiO_2	0.30	0.35	0.40	0.49	0.45	0.25	0.26	0.31
Al_2O_3	11.85	11.56	14.74	14.32	13.74	9.26	12.39	14.98
FeO	7.61	8.06	6.49	7.11	8.25	6.77	7.04	7.82
MnO	0.19	0.21	0.06	0.12	0.14	0.24	0.13	0.17
MgO	9.37	9.62	7.20	5.85	7.95	11.04	10.29	7.71
CaO	12.36	12.35	11.28	10.49	11.69	11.96	11.57	11.22
Na_2O	1.23	1.25	1.54	1.86	1.76	1.17	1.36	1.37
K_2O	0.24	0.16	0.23	0.26	0.24	0.27	0.28	0.28
H_2O	1.88	2.37	2.94	2.19	2.73	3.03	3.22	2.74
Total	97.51	99.48	100.09	98.51	100.55	99.39	101.14	98.07
Clinopyroxene								
SiO_2	53.94	53.91	53.95	52.66	53.98	55.11	55.48	54.19
TiO_2	0.07	0.06	0.08	0.12	0.12	0.05	0.4	0.07
Al_2O_3	1.15	1.21	1.52	1.51	1.55	0.65	0.89	1.94
FeO	3.07	3.34	3.61	4.59	3.89	2.69	3.20	4.61
MnO	0.05	0.16	0.13	0.16	0.09	0.03	0.02	0.13
MgO	19.34	19.15	18.82	17.97	18.75	19.96	19.59	18.84
CaO	21.04	20.17	21.24	20.29	21.01	20.78	20.48	19.99
Na_2O	0.13	0.14	0.11	0.12	0.12	0.14	0.11	0.14
Cr_2O_3	0.73	0.82	0.31	0.47	0.54	0.72	0.30	0.33
Total	99.52	98.96	99.77	97.89	100.05	100.13	100.11	100.24
Mg#	0.92	0.91	0.90	0.87	0.90	0.93	0.92	0.88
T, °C	1170	1165	1135	1110	1150	1180	1150	1130

Notes: H_2O was determined by the SIMS method; the oxides were analyzed by electron microprobe; *T* is homogenization temperature.
* Sample number here and in Table 3.

Table 3. Composition (ppm) of homogenized inclusions and host clinopyroxene: trace elements

Element	TRD-135/1	R, %	TRD-135/3	R, %	TRV-191/9	R, %	TRV-191/13	R, %	TRD-133/15	R, %
Clinopyroxene										
Ti	361	3.1	358	1.2	615	3.1	785	5.2	532	1.2
Sr	4.25	7.9	3.93	7.8	4.61	6.8	4.99	19.8	5.95	2.5
Y	1.31	6.7	1.35	9.8	3.00	10.2	4.59	1.0	2.14	4.2
Zr	0.52	6.8	0.54	2.3	0.82	10.7	1.44	8.9	0.70	15.1
Ba	0.045	90.9	0.049	61.1	0.024	107.2	0.050	51.8	0.012	74.8
La	0.018	23.2	0.025	19.5	0.031	24.6	0.048	13.0	0.032	16.2
Ce	0.096	26.7	0.093	25.4	0.152	10.0	0.266	5.9	0.182	11.9
Nd	0.167	16.3	0.148	24.3	0.366	10.0	0.550	13.3	0.373	3.1
Sm	0.118	14.0	0.091	39.4	0.241	13.9	0.321	9.9	0.124	20.3
Dy	0.253	9.4	0.246	5.3	0.560	11.9	0.861	4.3	0.418	6.0
Er	0.147	5.3	0.152	9.4	0.322	8.9	0.462	7.2	0.235	18.6
Yb	0.154	6.4	0.160	9.4	0.312	11.6	0.467	22.5	0.197	19.3
Inclusions										
Ti	1872	1.2	1869	1.2	2137	1.3	2876	0.8	2581	2.1
Sr	49.7	1.4	41.4	2.9	60.5	2.3	78.6	2.7	73.4	1.5
Y	7.56	3.6	8.15	1.4	8.32	3.3	12.49	4.6	10.37	4.6
Zr	12.5	2.1	12.4	4.2	14.5	3.8	27.1	3.8	21.7	9.0
Ba	17.8	6.3	15.0	3.7	14.3	7.7	29.0	11.8	18.9	2.0
La	0.66	8.6	0.66	10.4	0.63	7.3	1.76	10.7	1.13	6.9
Ce	1.82	5.5	1.72	12.1	1.89	7.4	4.66	11.3	3.12	10.5
Nd	1.67	13.3	1.61	10.4	1.82	7.1	3.75	13.1	2.92	10.6
Sm	0.70	8.6	0.72	8.4	0.69	19.8	1.30	5.2	1.17	7.5
Dy	1.28	12.2	1.46	5.9	1.50	11.1	2.52	5.4	1.77	10.0
Er	0.78	10.0	0.77	14.1	0.81	9.1	1.53	5.8	1.11	8.4
Yb	1.02	7.1	0.96	11.3	1.04	16.3	1.69	12.6	1.16	13.8
K_d										
Ti	0.193	3.4	0.192	1.7	0.288	3.4	0.273	5.3	0.206	2.4
Sr	0.085	8.0	0.095	8.3	0.076	7.2	0.063	19.9	0.081	2.9
Y	0.174	7.6	0.166	9.9	0.360	10.7	0.368	4.7	0.206	6.2
Zr	0.042	7.1	0.044	4.8	0.057	11.4	0.053	9.7	0.032	17.6
Ba	0.003	91.1	0.003	61.2	0.002	107.5	0.002	53.1	0.001	74.8
La	0.027	24.7	0.039	22.1	0.049	25.6	0.027	16.9	0.028	17.6
Ce	0.053	27.2	0.054	28.2	0.081	12.4	0.057	12.7	0.058	15.9
Nd	0.100	21.0	0.092	26.4	0.201	12.2	0.147	18.7	0.128	11.1
Sm	0.167	16.5	0.127	40.3	0.351	24.2	0.246	11.2	0.107	21.7
Dy	0.197	15.4	0.169	7.9	0.374	16.3	0.342	6.9	0.236	11.7
Er	0.188	11.3	0.198	16.9	0.399	12.7	0.302	9.2	0.212	20.4
Yb	0.151	9.5	0.167	14.7	0.299	20.0	0.276	25.8	0.169	23.7

TRV-200/16	R, %	TRV-200/19	R, %	TRV-200/20	R, %		
219	2.0	300	7.3	511	3.3		
6.69	6.5	6.02	6.2	5.37	4.4		
0.67	7.9	1.37	7.5	2.73	9.6		
0.42	11.1	0.47	18.3	1.02	5.3		
0.013	66.1	0.038	58.4	0.028	12.4		
0.015	25.7	0.032	35.9	0.036	20.5		
0.075	10.4	0.113	18.3	0.171	4.3		
0.125	4.2	0.181	6.8	0.350	11.6		
0.089	15.9	0.129	2.6	0.267	8.6		
0.132	8.5	0.261	15.4	0.543	3.2		
0.077	26.4	0.165	35.0	0.332	16.8		
0.082	17.3	0.157	20.6	0.325	10.2		
1329	1.2	1460	1.5	1639	1.4		
63.7	0.7	78.0	1.3	75.9	3.3		
5.69	4.9	6.52	5.9	7.65	4.2		
13.4	2.3	14.8	3.3	13.9	5.5		
15.9	1.9	15.2	4.8	13.8	4.9		
0.98	7.7	1.08	22.4	0.88	11.0		
2.28	6.4	2.57	4.4	2.28	6.3		
1.61	9.6	2.04	7.6	1.77	8.1		
0.55	12.4	0.71	20.5	0.77	21.1		
1.03	9.8	1.27	11.5	1.36	10.4		
0.59	9.1	0.75	8.5	0.79	8.5		
0.69	2.6	0.81	10.0	0.95	7.3		
						Average K_d	**R, %**
0.165	2.4	0.206	7.4	0.312	3.6	0.229	23.4
0.105	6.6	0.077	6.4	0.071	5.5	0.082	16.3
0.117	9.2	0.210	9.5	0.357	10.5	0.245	41.2
0.032	11.3	0.032	18.6	0.074	7.6	0.046	32.7
0.001	66.1	0.002	58.6	0.002	13.3	0.002	46.6
0.015	26.8	0.030	42.3	0.041	23.2	0.032	32.5
0.033	12.2	0.044	18.8	0.075	7.6	0.057	27.0
0.078	10.5	0.089	10.2	0.197	14.1	0.129	37.9
0.162	20.1	0.181	20.7	0.345	22.8	0.211	44.7
0.128	13.0	0.206	19.2	0.399	10.9	0.256	39.6
0.131	27.9	0.22	36.0	0.421	18.8	0.259	40.4
0.118	17.5	0.195	22.9	0.341	12.5	0.214	37.4

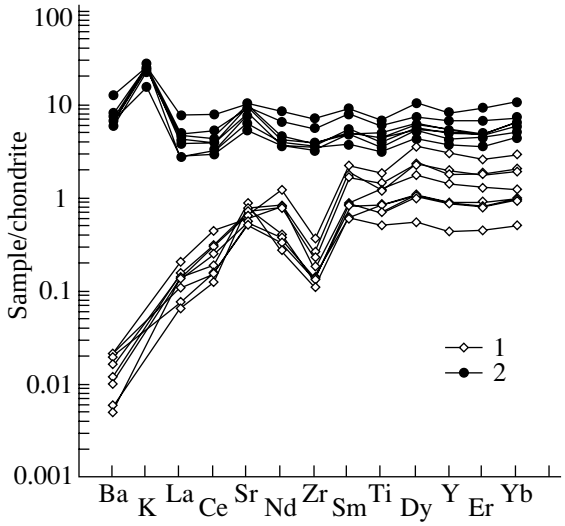

Fig. 4. Normalized contents of incompatible elements in clinopyroxenes (1) and melt inclusions (2).
The element contents were normalized to chondrite after Anders and Grevess (1989).

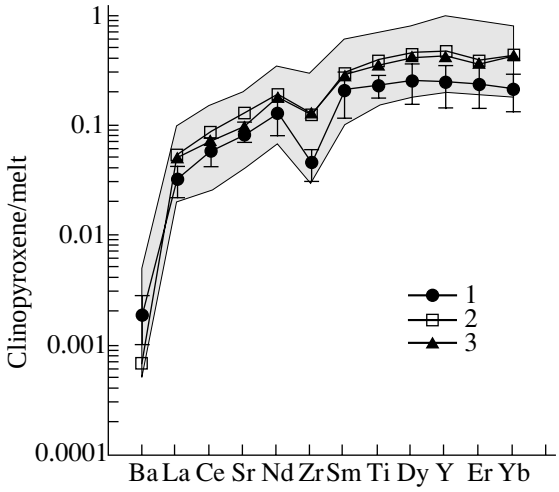

Fig. 5. Average partition coefficients between clinopyroxene and melt.
1—our data; 2—data of Hart and Dunn (1993); 3—data of Johnson (1994). Shown as a field is the distribution coefficient range for clinopyroxene reported by Green (1994).

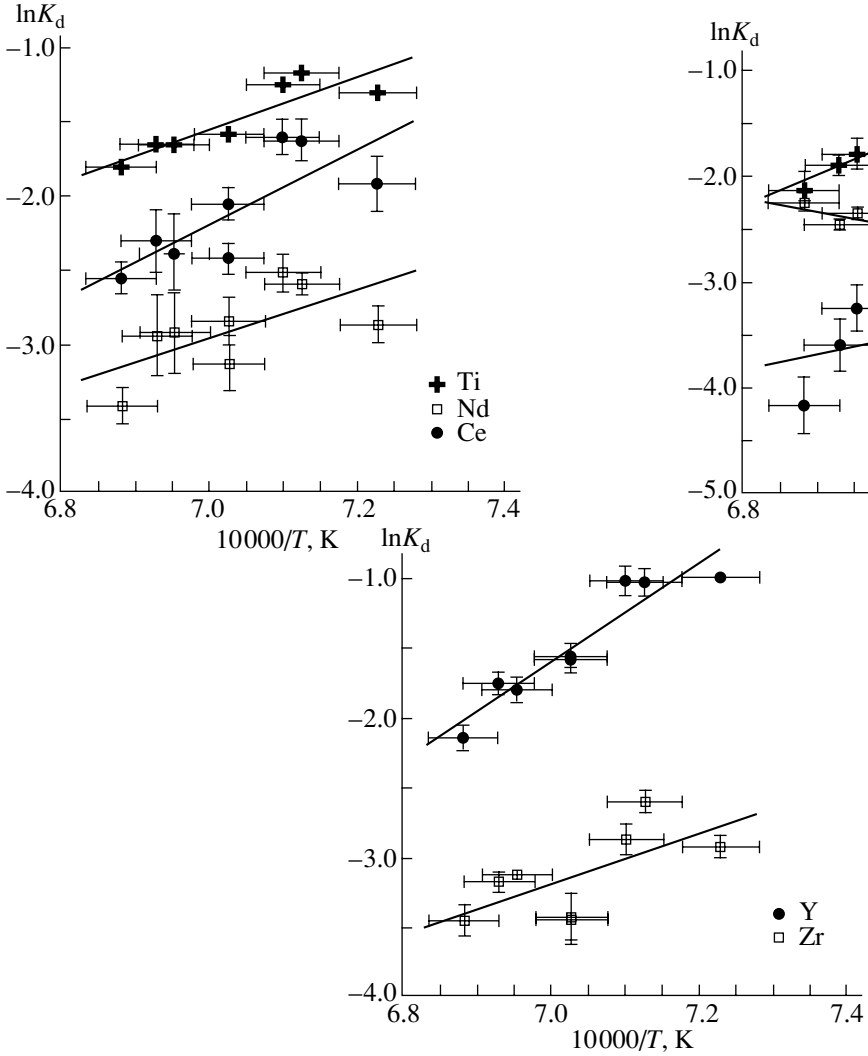

Fig. 6. Temperature variation of partition coefficients for select elements.

The trends for all elements but Sr are subparallel. The slopes of the lines, however, are seen to increase regularly with the decreasing incompatibility of the elements with the melt. This fact is demonstrated in Fig. 7, which shows correlation between coefficient A and the REE ionic radii. The relationship is fairly well described by the linear regression equation (R = 0.91). This indicates that the temperature relationship varies with the crystal chemistry of the elements.

As follows from Fig. 8, the K_d values found for all elements except Ba show a significant linear correlation with the Al_2O_3 content of the clinopyroxene: the K_d values increase with the increasing Al_2O_3 contents in the clinopyroxene for most of the elements (except Sr). It is possible that this relationship is responsible for our systematically lower K_d values compared with the values obtained for substantially more aluminous clinopyroxenes in high-temperature and high-pressure experiments (Fig. 5).

The abnormal K_d behavior for Sr (Figs. 6, 8) revealed that Sr is the only element, for which the K_d value increases with increasing temperature and the decreasing alumina content of the clinopyroxene.

Table 4. Parameters of K_d variation with temperature

Element	A	ΔA	B	ΔB	R
La	1.42	1.11	–13.51	7.78	0.47
Ce	1.58	0.77	–14.01	5.43	0.64
Nd	2.48	0.82	–19.59	5.79	0.78
Sm	2.41	1.20	–18.61	8.48	0.63
Dy	3.17	0.65	–23.71	4.58	0.89
Er	2.79	0.75	–21.16	5.29	0.84
Yb	2.88	0.61	–21.85	4.27	0.89
Ba	0.38	2.02	–9.04	14.19	0.08
Y	3.50	0.51	–26.08	3.57	0.94
Ti	1.76	0.38	–13.84	2.67	0.88
Sr	–1.32	0.18	6.79	1.27	0.95
Zr	1.76	0.84	–15.52	5.92	0.65

Note: A and B are linear regression coefficients in the equation $K_d = A \times 10000/(T, K) + B$; ΔA and ΔB are standard errors; R is correlation coefficient. The underlined R values exceed the critical value for 5% significance level (R = 0.707 for $n = 8$).

DISCUSSION OF RESULTS

The results of this study are limited in terms of the amount of data used and the range of clinopyroxene and melt compositions. For this reason, the K_d values obtained can be used in numerical calculations within the narrow range of temperatures and compositions investigated. More universal relationships call for further studies with wider composition and temperature ranges. Furthermore, K_d should be described as an equilibrium constant in a more rigorous thermodynamic form using the activities of components in the melt and pyroxenes. Such models have been described in the literature (e.g., Hack *et al*., 1994), but unfortunately, none of them can be applied to our data because they were designed for anhydrous melts and substantially more aluminous pyroxenes.

Nevertheless, the results of our study permit the conclusion that this method of K_d evaluation holds promise for the future. This conclusion is based on the following facts:

(1) The K_d values determined for all the elements concerned fit within the range of values found by other methods and reproduce the known features of the K_d behavior in the series of element incompatibility (Fig. 5);

(2) The K_d values show significant correlations with equilibrium temperatures for most of the elements, these correlations being consistent with data from the literature (Fig. 6);

(3) A relationship has been established between the K_d variation with temperature and the crystal chemistry of REE elements (Fig. 7).

The abnormal behavior of Sr in terms of its K_d variation with temperature and the alumina content of clinopyroxene, compared with elements of similar incompatibility with the melt (Ce, Nd), justifies the prediction of positive Sr anomalies in relatively high-temperature, low-Al mantle clinopyroxenes. Such clinopyroxenes have been reported from highly depleted abyssal peridotites found in hot-spot areas associated with mid-ocean ridges (Johnson *et al*., 1990).

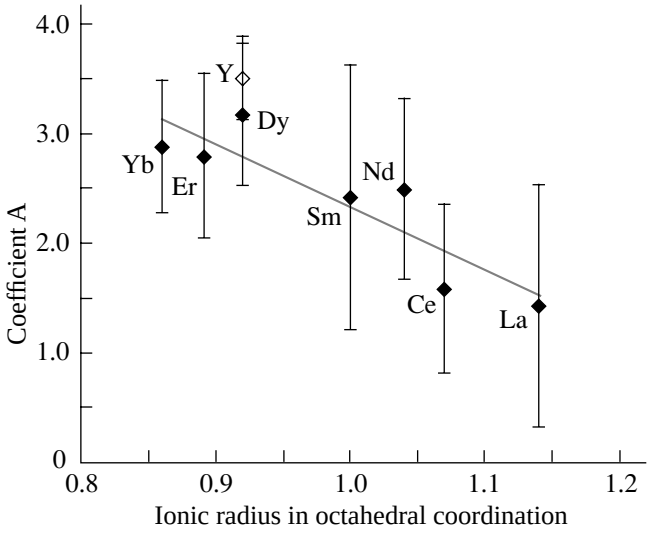

Fig. 7. Variation of the temperature-dependent K_d values for REE and Y as a function of their crystal chemistry.

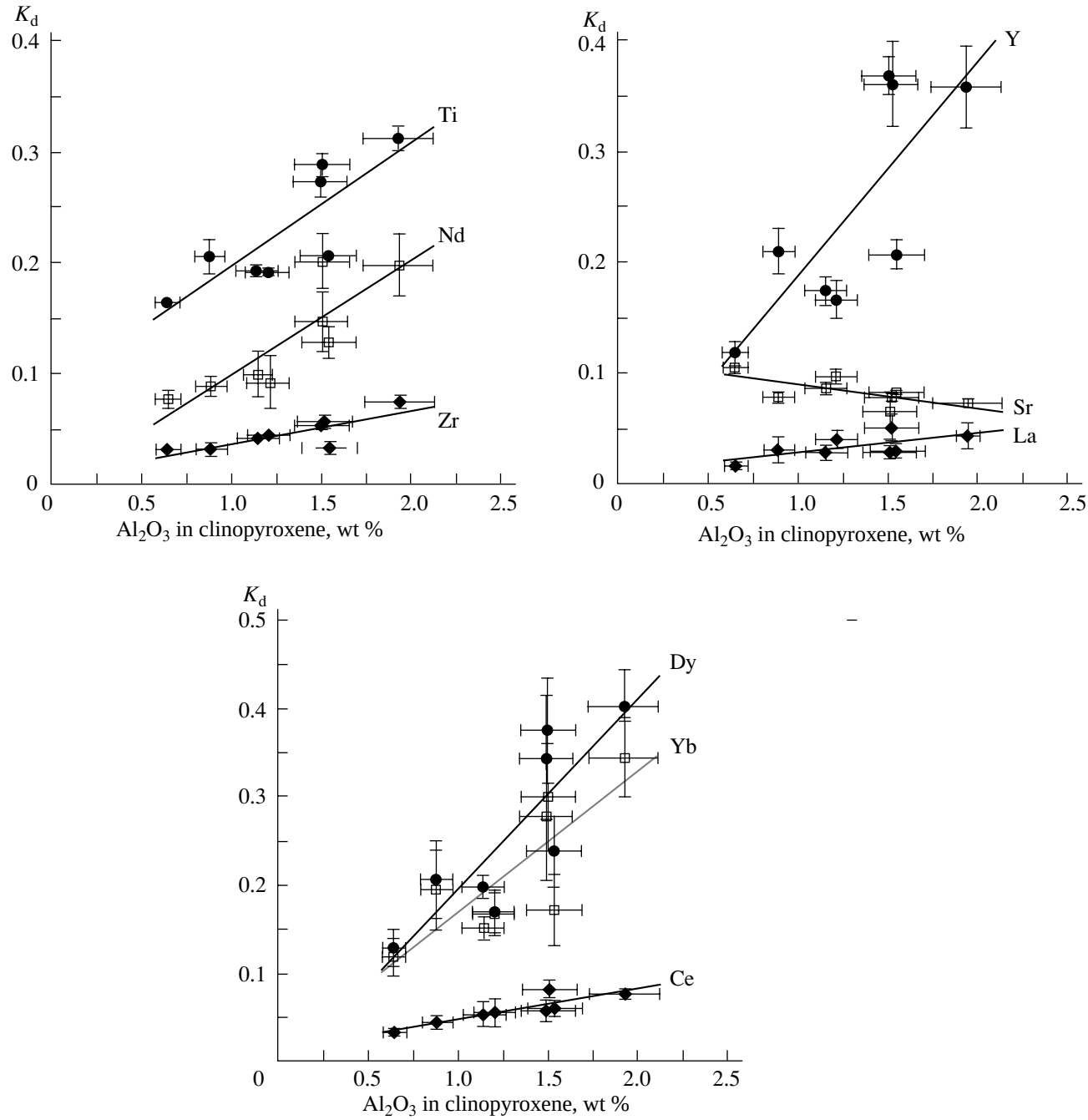

Fig. 8. Variation of partition coefficients as a function of clinopyroxene composition.

CONCLUSION

1. Melt inclusions in clinopyroxene from the Troodos lavas were studied using the methods of high-temperature optical thermometry, secondary ion mass spectrometry, and electron probe microanalysis. The partitioning coefficients of Ba, Sr, Y, Ti, La, Ce, Nd, Sm, Dy, Er, and Yb between low-Al, high-Mg clinopyroxene and boninite-like melt were determined for temperatures of 1100–1190°C and hydrous fluid pressure of 1 kbar.

2. Relationships were established between the partition coefficients of incompatible elements and the temperature and alumina content of clinopyroxene.

3. The results prove that the study of melt inclusions in minerals offers promise as an efficient tool for determining the partition coefficients of trace elements between the crystalline phase and melt.

ACKNOWLEDGMENTS

We are grateful to S.A. Simakin and N.N. Kononkova for carrying out ion and electron microprobe analyses, respectively. This work was done with the financial support of the International Science Foundation (grants MNN000 and MNN300), the Volkswagen Stiftung Foundation (grant I/68-569), and the Russian Foundation for Basic Research (projects nos. 93-058895 and 96-05-66014).

REFERENCES

Anders, E. and Grevess, N., Abundance of the Elements: Meteoritic and Solar, *Geochim. Cosmochim. Acta*, 1989, vol. 53, no. 1, pp. 197–214.

Batanova, V.G., Sobolev, A.V., and Schmincke, H.-U., The Parent Magmas of Intrusive Cumulates from the Troodos Massif, Cyprus: A Comparative Study of Clinopyroxenes and Melt Inclusions in Plagioclase, *Petrologiya*, 1996, vol. 4, no. 3.

Burnham, C.W., Water and Magmas: A Mixing Model, *Geochim. Cosmochim. Acta*, 1975, vol. 39, pp. 1077–1082.

Czamanske, G.K., Sisson, T.W., Campbell, J.L., *et al.*, Micro-PIXE Analysis of Silicate Reference Standards, *Am. Mineral.*, 1993, vol. 78, pp. 893–903.

Green, T.H., Experimental Studies of Trace Element Partitioning Applicable to Igneous Petrogenesis—Sedona 16 Years Later, *Chem. Geol.*, 1994, vol. 117, pp. 1–36.

Hack, P.J., Nielsen, R.J., and Johnston, A.D., Experimentally Determined Rare-Earth Element and Y Partitioning Behavior between Clinopyroxene and Basaltic Liquids at Pressure up to 20 kbar, *Chem. Geol.*, 1994, vol. 117, pp. 89–105.

Hart, S.R. and Dunn, T., Experimental *Cpx*/Melt Partitioning of 24 Trace Elements, *Contrib. Mineral. Petrol.*, 1993, vol. 113, pp. 1–8.

Jarosewich, E.J., Nelen, J.A., and Norberg, J.A., Reference Samples for Electron Microprobe Analysis, *Geostand. Newsl.*, 1980, vol. 4, pp. 43–47.

Johnson, K.T.M., Experimental *Cpx*/ and Garnet/Melt Partitioning of REE and Other Trace Elements at High Pressures: Petrogenetic Implications, *Mineral. Mag.*, 1994, vol. 58A, pp. 454–455.

Johnson, K.T.M. and Dick, H.J.B., Open System Melting and Temporal and Spatial Variation of Peridotite and Basalts at the Atlantis II Fracture Zone, *J. Geophys. Res.*, 1992, vol. 97, no. B6, pp. 9219–9241.

Johnson, K.T.M., Dick, H.J.B., and Shimizu, H., Melting in the Oceanic Upper Mantle: An Ion Microprobe Study of Diopsides in Abyssal Peridotites, *J. Geophys. Res.*, 1990, vol. 95, pp. 2661–2678.

Navon, O. and Stolper, E., Geochemical Consequences of Melt Percolation: The Upper Mantle As a Chromatographic Column, *J. Geol.*, 1987, vol. 95, no. 3, pp. 285–307.

Nielsen, R.L. and Drake, M.J., Pyroxene–Melt Equilibria, *Geochim. Cosmochim. Acta*, 1979, vol. 43, pp. 1259–1272.

Nimis, P., A Clinopyroxene Geobarometer for Basaltic Systems in Crystal-Structure Modeling, *Contrib. Mineral. Petrol.*, 1995, vol. 121, pp. 115–125.

Portnyagin, M.V., Magakyan, R., and Schmincke, H.-U., Geochemical Variability of Boninite Magmas: Evidence from Magmatic Inclusions in Highly Magnesian Olivine from Lavas of Southwestern Cyprus, *Petrologiya*, 1996, vol. 4, no. 3, pp. 250–265.

Roedder, E., Fluid Inclusions, *Mineral. Soc. Am.*, 1984, vol. 14.

Sobolev, A.V., Melt Inclusions in Minerals—A Source of Principal Petrological Information, *Petrologiya*, 1996, vol. 4, no. 3.

Sobolev, A.V. and Batanova, V.G., Mantle Lherzolites of the Troodos Ophiolite Complex, Cyprus: Clinopyroxene Geochemistry, *Petrologiya*, 1995, vol. 3, no. 5, pp. 487–495.

Sobolev, A.V. and Danyushevsky, L.V., Petrology and Geochemistry of Boninites from the North Termination of the Tonga Trench: Constraints on the Generation Conditions of Primary High-Ca Boninite Magmas, *J. Petrol.*, 1994, vol. 35, pp. 1183–1211.

Sobolev, A.V., Portnyagin, M.V., Dmitriev, L.V., *et al.*, Petrology of Ultramafic Lavas and Associated Rocks of the Troodos Massif, Cyprus, *Petrologiya*, 1993, vol. 1, no. 4, pp. 379–412.

Sobolev, A.V. and Shimizu, N., Ultradepleted Primary Melt Included in an Olivine from the Mid-Atlantic Ridge, *Nature*, 1993, vol. 363, no. 6425, pp. 151–154.

Urusov, V.S. and Dudnikova, V.B., A Mechanism for the Growth of Trace Element Distribution Coefficient in Crystallization Processes (Capture Effect): Isovalent Systems, *Geokhimiya*, 1993, no. 4, pp. 499–513.

Wood, B. and Fraser, D., *Elementary Thermodynamics for Geologists*, Oxford (UK): Oxford Univ., 1977.